

# A Resource Efficient Source of Multi-photon Polarization Entanglement

E. Megidish, T. Shacham, A. Halevy, L. Dovrat, and H. S. Eisenberg

*Racah Institute of Physics, Hebrew University of Jerusalem, Jerusalem 91904, Israel*

Current photon entangling schemes require resources that grow with the photon number. We present a new approach that generates quantum entanglement between many photons, using only a single source of entangled photon pairs. The different spatial modes, one for each photon as required by other schemes, are replaced by different time slots of only two spatial modes. States of any number of photons are generated with the same setup, solving the scalability problem caused by the previous need for extra resources. Consequently, entangled photon states of larger numbers than before are practically realizable.

PACS numbers: 03.67.Bg, 42.50.Dv

The generation of quantum entangled states of many particles is a central goal of quantum information science. These states are required for the one-way quantum computer scheme [1, 2]. In quantum communication, they enable error correction [3] and multi-party protocols [4, 5]. Additionally, they can refute local realistic theories with an increasing violation as the particle number increases [6–8].

Polarized photons are an attractive realization of qubits due to their simple single-qubit operations and their weak interaction with the environment. Pairs of polarization entangled photons are easily generated by using the nonlinear optical effect of parametric down-conversion (PDC) [9]. Difficulties are encountered when trying to entangle more than two photons. Eight photons have already been entangled in a GHZ state [10–12], and six photons in an H-shaped graph [13] and Dicke [14] states. Currently, the state with the largest number of entangled particles of any realization is a GHZ state composed of 14 ions trapped in a linear trap [15].

In previous experiments, two polarization-entangled photon pairs were fused into a four-photon GHZ state by a polarizing beam-splitter (PBS) [16] (see Fig. 1a). A PBS is an optical element that transmits horizontally ( $h$ ) polarized photons and reflects them when vertically polarized ( $v$ ). Assuming an entangled pair in the  $|\phi^+\rangle$  Bell state [9] in paths 1 and 2, and another one in paths 3 and 4, the four-photon state is:

$$|\phi_{12}^+\rangle \otimes |\phi_{34}^+\rangle = \frac{1}{2}(|h_1 h_2\rangle + |v_1 v_2\rangle) \otimes (|h_3 h_4\rangle + |v_3 v_4\rangle). \quad (1)$$

If paths 2 and 3 are combined at a PBS, and we demand that one photon comes out of each of the two output ports, only the two amplitudes with identical polarizations in these modes are left and the result is a four-photon GHZ state:

$$|\Psi_{GHZ}^{(4)}\rangle = \frac{1}{\sqrt{2}}(|h_1 h_2 h_3 h_4\rangle + |v_1 v_2 v_3 v_4\rangle). \quad (2)$$

There is a strict requirement for the combined paths to be indistinguishable in all degrees of freedom, in order for

their amplitudes to interfere. Temporal indistinguishability is satisfied by generating the photons with a pulsed laser that defines their generation time, and carefully matching their relative path lengths. Fortunately, there is no need for sensitive phase accuracy, but just an overlap of the pulse envelopes.

This scheme is extendable in a straight forward manner. For example, if a third entangled photon-pair is added in paths 5 and 6, another PBS can fuse it by combining paths 4 and 5 to create a six-photon GHZ state [13] (see Fig. 1a). The addition of each extra pair requires another passage of the pump beam through a generating crystal, the adjustment of an additional delay line, an additional projecting PBS and a detection setup that includes two additional PBS elements and four more single-photon detectors. Clearly, this approach is non-scalable in material resources. Another issue is the non-scalability in temporal resources. Such experiments typically have an entangled-photon-pair generation probability of one pair every 100 pump pulses and an overall single-photon detection efficiency of 10-25%. Thus, the more photons an experiment is trying to produce, the longer the time it takes to accumulate sufficient data statistics.

In this Letter, we suggest a new approach that solves the problem of scalability with material resources. Our scheme uses only a single entangled photon-pair source, a single delay line and a single projecting PBS element to create entangled states of any number of photons. A pump pulse is down-converted in a nonlinear crystal. When a polarization entangled photon pair is generated, the right photon is directed to a PBS (see Fig. 1b), while the left photon enters a delay line. The delay time  $\tau$  is chosen such that if a second entangled photon pair is created by the next pump pulse, the right photon of the second pair meets with the left photon of the first pair at the projecting PBS. Post-selecting the events in which one photon exits at each PBS output port, projects the two entangled pairs onto a four-photon GHZ state. The left photon of the second pair arrives at the PBS after travelling through the delay line. The four spatial modes of previous schemes [16] (1, 2, 3 and 4, as in Eq. 2) are

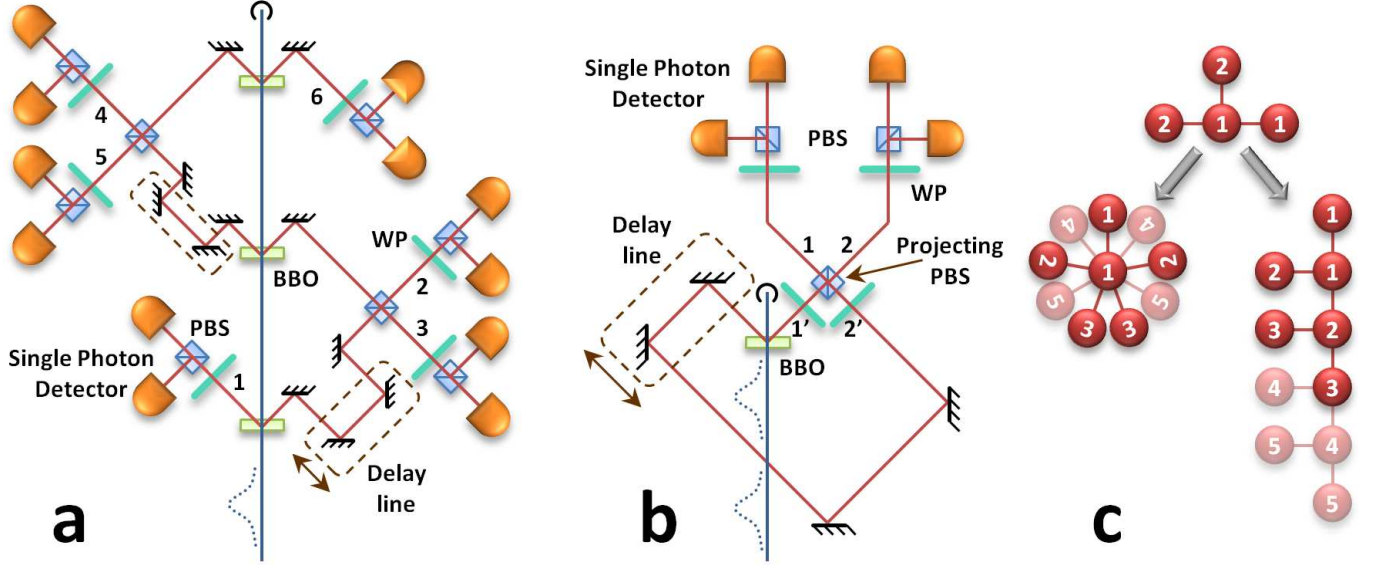


FIG. 1. (Color online) A comparison between previous setups and our setup. (a) The previously used setup for entangling four and six photons in a GHZ state. Three  $\beta$ -BaB<sub>2</sub>O<sub>4</sub> (BBO) crystals generate from a single pump pulse three entangled photon pairs in six spatial modes. Delay lines synchronize the projection of a photon from each pair onto a PBS. Six analyzing wave-plates (WP), six PBS's and twelve detectors are required to measure the state. To produce eight photon entanglement, this setup needs additional components. (b) Our resource efficient setup. Only a single crystal generates pairs from many pump pulses. The pairs are projected onto a large entangled state on a single PBS and occupy two spatial modes and additional temporal modes. The same setup is applicable to entanglement generation of any photon number. (c) The two multi-photon entangled graph states that are possible to obtain without fast polarization rotations: a growing star shaped GHZ state and a connected branched chain (which for 3 pairs is an H-graph state). For two photon pairs, both states are identical. Numbered circles mark photons and their creation order, where dimmed circles represent possible future states of 4 and 5 fused pairs. Connecting lines mark the entangling operations that define the quantum graph state.

replaced by two spatial modes (1 and 2 after the projecting PBS, 1' and 2' before it) and three temporal modes (0,  $\tau$ , and  $2\tau$ ):

$$|\Psi_{GHZ}^{(4)}\rangle = \frac{1}{\sqrt{2}}(|h_1^0 h_2^\tau h_1^\tau h_2^{2\tau}\rangle + |v_1^0 v_2^\tau v_1^\tau v_2^{2\tau}\rangle), \quad (3)$$

where the lower and upper indices designate the spatial and the temporal modes, respectively. The first and last photons are considered before the projecting PBS. It is possible to convert the mixed spatio-temporal mode partition to only spatial modes by fast polarization-independent switches.

The most important point to note is the result of the generation of a third entangled photon pair from the next pump pulse. The right photon of this third pair is entangled at the PBS with the delayed left photon of the second pair. All of the six photons from the three pairs are now in a six-photon GHZ state. There is no need for any modification between the setups that create the four- and the six-photon entangled states. It is also clear by induction that as long as additional consecutive pairs are created, larger entangled states can be produced.

The use of a PDC source is merely for demonstration purposes, as our approach can use any photon entangling source, current or futuristic [17–19]. Therefore, our

scheme does neither address the probabilistic nature of PDC sources, nor other issues that these sources raise, such as the spectral distinguishability between different photon pairs [20]. Nevertheless, our scheme greatly simplifies the standard approach, enabling the demonstration of entangled photon states of high photon numbers.

In order to demonstrate our scheme, we created polarization entangled photon pairs by the nonlinear type-II parametric down-conversion process [9]. A pulsed Ti:Sapphire laser source with a 76 MHz repetition rate is frequency doubled to a wavelength of 390 nm and an average power of 400 mW. The laser beam is corrected for astigmatism and focused on a 2 mm thick  $\beta$ -BaB<sub>2</sub>O<sub>4</sub> (BBO) crystal. Down-converted photons, with a wavelength of 780 nm, are spatially filtered by coupling them into and out of single-mode fibers, and spectrally filtered by 3 nm wide bandpass filters.

The delay length is chosen such that it fuses pairs that are created eight pulses apart. The delay time is 105 ns, which is longer than the dead time of 50 ns of the single-photon detectors (Perkin Elmer SPCM-AQ4C). The delay line is a free-space delay line (31.6 m long), built from high reflecting dielectric mirrors. The total transmittance is higher than 90% after 10 reflections. The delay line was designed to cancel distinguishability that results

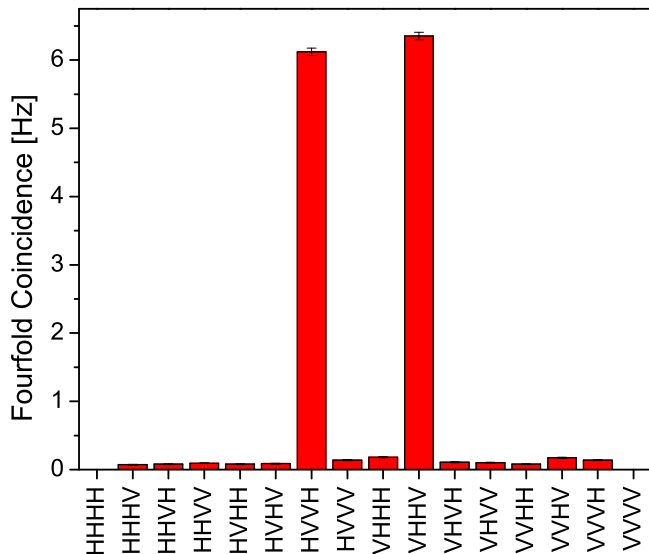


FIG. 2. (Color online) Measured amplitude histogram of the generated four-photon GHZ state. Two opposite amplitudes occur on average 65 times more often than any other amplitude. Data was accumulated over 2000 sec. We used photon pairs in the  $|\psi^+\rangle$  Bell state. The results are equivalent to using a  $|\phi^+\rangle$  state, up to local polarization rotations.

from the different beam propagation properties of the short and long paths.

In order to characterize the four-photon state, the four-photon correlation statistics in the **HV** (horizontal-vertical polarization) basis was measured (see Fig. 2). Two opposite possibilities (**HVVH** and **VHHV**) are much more probable than the others, as expected from a four-photon GHZ state. Additionally, measurements in a rotated polarization basis (plus and minus (**PM**)  $45^\circ$  linear or right and left (**RL**) circular) are required in order to demonstrate the coherence between these two amplitudes. After rotation, there are 16 possible amplitudes, divided into two groups: the even and the odd amplitude groups, where each polarization appears an even or an odd number of times, respectively. When the two projected photons are indistinguishable, one of the amplitude groups interferes constructively and the other destructively (which one depends on the specific polarization rotations).

The two projected photons can be rotated individually with wave plates positioned after the PBS projection. As the first and last photons are actually measured at the projecting PBS, it would seem that fast Pockels cells would need to be placed before this PBS in order to rotate them. Fortunately, there is a way to circumvent this complication. If the phase of the entangled pairs is tuned to  $90^\circ$  such that their state becomes

$$|\phi^i\rangle = \frac{1}{\sqrt{2}}(|h_1 h_2\rangle + i|v_1 v_2\rangle), \quad (4)$$

and half-wave plates at  $22.5^\circ$  are positioned before the

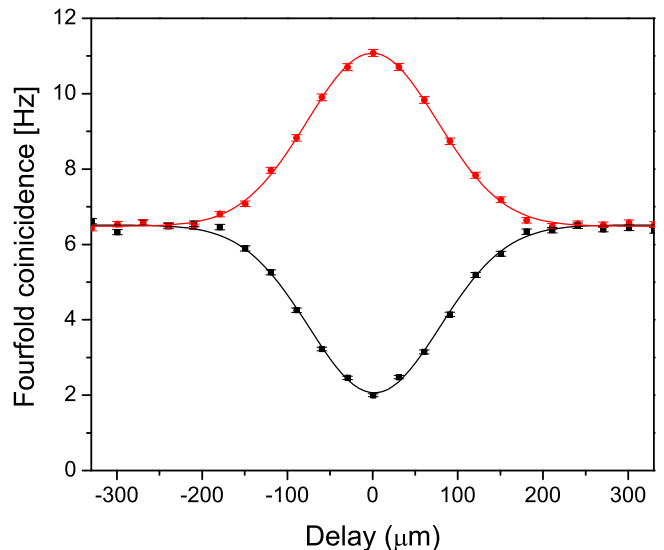


FIG. 3. (Color online) Coherence of the GHZ state. The sum of all even amplitudes (black squares) and the sum of all odd amplitudes (red circles) at a rotated polarization basis vs. the relative delay between the short and the long paths. At zero delay, the even amplitudes interfere destructively and the odd amplitudes interfere constructively. When delay is introduced, the two GHZ amplitudes are temporally distinguishable and interference is lost. The interference visibility is  $69.5 \pm 0.8\%$ . Data was accumulated over 480 sec per point.

projecting PBS, the polarization of the first and last photons is non-locally rotated before the PBS to the circular polarization basis while that of the two projected photons remains unchanged (see the Supplemental Material for a detailed calculation for this rotation [21]).

We applied these rotations and detected all of the 16 even and odd amplitudes. Each possibility corresponds to different sequences of the four detectors. Programmable electronics is used to register the various sequences. The overall post-selected four-photon rate is 13 events per second. Figure 3 presents the sums of all counts of the 8 even and of the 8 odd amplitudes (showing destructive and constructive interference, respectively), as the delay length is scanned. Figure 4 presents the 16 amplitudes that Fig. 3 is composed of. There are enough events to observe the interference of all single amplitudes. The threshold visibility required for the demonstration of non-locality with four particles is below 35% [6, 7]. The observed interference visibility here is  $69.5 \pm 0.8\%$ . As the two-photon visibilities are relatively high (larger than 90% for HV, PM, and RL measurement bases at low pump power), the four-photon visibility is an indication for the projection quality. Nevertheless, the entangled-pair quality is still a major cause for the fourfold visibility degradation. We estimate the effect of higher order terms to cause a degradation of only  $\sim 3\%$ .

The fidelity with a GHZ state can be estimated from the histogram data of Fig. 2 and the observed fourfold

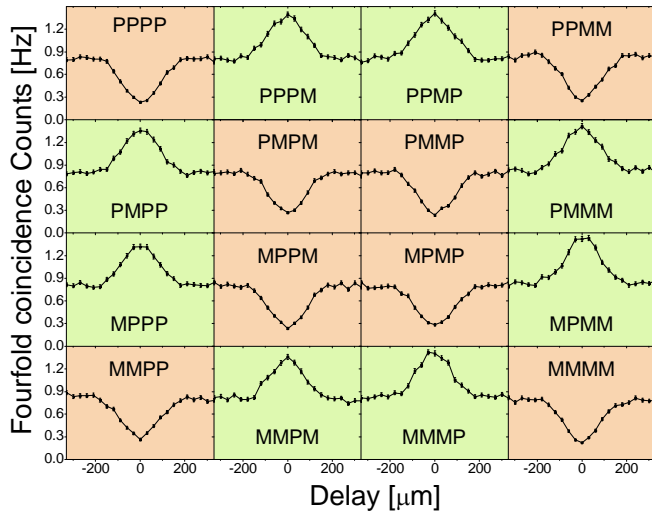


FIG. 4. (Color online) Fourfold coincidence counts of the 16 individual amplitudes of four photons at the plus-minus  $45^\circ$  (PM) linear polarization basis. At zero delay, counts from all odd amplitudes (light green background) increase while counts from all even amplitudes (light orange background) decrease. Figure 3 is composed of these scans.

visibility. The worst case of full coherence between the unwanted diagonal elements of the state density matrix yields a lower bound of 75.2% fidelity and assuming no coherence between these terms results in 79.9%. As the observed fidelity is higher than 50%, it is clear evidence of genuine quantum entanglement between the generated four photons. We see continuous improvement of the fourfold visibility and the fidelity as the setup is technically improved. See the Supplemental Material for a detailed description of the causes for visibility degradation [21].

As the same setup can generate six-photon entanglement, we used it to detect six-photon states and recorded 30 sixfold events per hour for a pump power of 500 mW. As all of the entangled pairs are produced by the same source, all three pairs have identical quantum properties. The PBS entangling operations between the first and second pairs and between the second and third pairs are identical. Therefore, measuring genuine entanglement between four photons indicates that entanglement exists between all of the six detected photons. Quantifying the amount of sixfold entanglement is left for a future work.

As long as additional pairs are being entangled, a larger GHZ state is created. Interestingly, when fusing  $|\phi^i\rangle$  pair states (Eq. 4) instead of  $|\phi^+\rangle$ , the growing state is described by a different type of graph from the GHZ graph [22] (see Fig. 1c). The four-photon state is still a GHZ state, but the six-photon state is an H-graph state [13] (Fig. 1c), as the left photon from the second pulse is projected on the PBS after already being rotated to the PM basis. When yet another (fourth) pair is entangled, the sixth photon is also rotated, and this pair branches

from a corner of the H-graph.

To conclude, we have demonstrated a new scheme for the generation of entanglement between many photons. It is efficient in the required material resources, as the same setup can entangle any number of photons, without any change. Hence, our scheme can enable the demonstration of states with larger photon numbers than what is practically realizable today. Similar to other available schemes, our scheme suffers from decreasing state production rate with the number of photons. Nevertheless, there is much room for improvement as the photon-pair generation probability is currently between 1 – 2%, but up to 10% is acceptable (see Supplemental Material [21]). Photon numbers can be further increased by using a pump laser with higher power [12], a generating crystal with higher nonlinear coefficients [23], improving photon collection [24] and detection [25] efficiencies, using detectors with shorter dead times [26, 27], lasers with higher repetition rates [28] and the coherent addition of pump pulses [29]. More virtual qubits can be added to the generated state by using hyper-entanglement [30], resulting in states of more connected graphs and higher quantum Hilbert spaces [31]. The incorporation of fast polarization rotations will enable the generation of different graph states, as well as on-the-fly alteration of the measurement basis according to previous measurement outcomes, a procedure known as *feed-forward* [32] which is required for one-way quantum computation [1].

The authors thank the Israeli Science Foundation for supporting this work under grants 366/06 and 546/10.

- 
- [1] R. Raussendorf and H.-J. Briegel, Phys. Rev. Lett. **86**, 5188 (2001).
  - [2] P. Walther *et al.*, Nature **434**, 169 (2005).
  - [3] D. Schlingemann and R. F. Werner, Phys. Rev. A **65**, 012308 (2001).
  - [4] M. Hillery, V. Buzek, and A. Berthiaume, Phys. Rev. A **59**, 1829 (1999).
  - [5] Z. Zhao *et al.*, Nature **430**, 54 (2004).
  - [6] N. D. Mermin, Phys. Rev. Lett. **65**, 1838 (1990).
  - [7] M. Żukowski and D. Kaszlikowski, Phys. Rev. A **56**, R1682 (1997).
  - [8] O. Gühne, G. Tóth, P. Hyllus, and H.-J. Briegel, Phys. Rev. Lett. **95**, 120405 (2005).
  - [9] P. G. Kwiat *et al.*, Phys. Rev. Lett. **75**, 4337 (1995).
  - [10] D. M. Greenberger, M. A. Horne, A. Shimony, and A. Zeilinger, Am. J. Phys. **58**, 1131 (1990).
  - [11] Y.-F. Huang *et al.*, Nature Comm. **2**, 546 (2011).
  - [12] X.-C. Yao *et al.*, Nature Photon. **6**, 225 (2012).
  - [13] C.-Y. Lu *et al.*, Nature Phys. **3**, 91 (2007).
  - [14] W. Wieczorek *et al.*, Phys. Rev. Lett. **103**, 020504 (2009).
  - [15] T. Monz *et al.*, Phys. Rev. Lett. **106**, 130506 (2011).
  - [16] J.-W. Pan, M. Daniell, S. Gasparoni, G. Weihs, and A. Zeilinger, Phys. Rev. Lett. **86**, 4435 (2001).
  - [17] N. Akopian *et al.*, Phys. Rev. Lett. **96**, 130501 (2006).

- [18] R.M. Stevenson *et al.*, Nature **439**, 179 (2006).
- [19] C. L. Salter *et al.*, Nature **465**, 594 (2010).
- [20] P. J. Mosley *et al.*, Phys. Rev. Lett. **100**, 133601 (2008).
- [21] See Supplemental Material at <http://>.
- [22] M. Hein, J. Eisert, and H.-J. Briegel, Phys. Rev. A **69**, 062311 (2004).
- [23] A. Halevy *et al.*, Opt. Express **19**, 20420 (2011).
- [24] C. Kurtsiefer, M. Oberparleiter, and H. Weinfurter, Phys. Rev. A **64**, 023802 (2001).
- [25] S. Takeuchi, J. Kim, Y. Yamamoto, and H. H. Hogue, App. Phys. Lett. **74**, 1063 (1999).
- [26] G. N. Gol'tsman *et al.*, Appl. Phys. Lett. **79**, 705 (2001).
- [27] P. Eraerds, M. Legré, A. Rochas, H. Zbinden, and N. Gisin, Opt. Express **15**, 14539 (2007).
- [28] A. Bartels, D. Heinecke, and S. A. Diddams, Opt. Lett. **33**, 1905 (2008).
- [29] R. Krischek *et al.*, Nature Photon. **4**, 170 (2010).
- [30] P. G. Kwiat and H. Weinfurter, Phys. Rev. A **58**, R2623 (1998).
- [31] W.-B. Gao *et al.*, Nature Phys. **6**, 331 (2010).
- [32] R. Prevedel *et al.*, Nature **445**, 65 (2007).